Laser micro Raman investigations on gas hydrates

P. S. R. Prasad*, K. Shiva Prasad, Y. Sowjanya and Kalachand Sain

Gas Hydrate Division, National Geophysical Research Institute, Hyderabad 500 007, India

Laser Raman spectroscopic measurements for some hydrocarbon gas molecules (propane and methane) have been reported on laboratory-synthesized hydrates in India. Our results corroborate the literature data, thus providing good laboratory standards. Such measurements are vital while analysing natural samples, where the guest molecules could be methane, ethane, propane, etc. The present results also demonstrate that the Raman mode around 60 cm^{-1} is a characteristic feature for structure-II hydrates. Gas hydrates with mixed guest molecules (tetrahydrofuran (THF) and methane) were also probed by Raman spectroscopy. The observed Raman spectra clearly indicate that the methane molecules occupy smaller cages upon using THF and water in 1 : 17 mol ratio. However, the Raman signatures for both large and small cages, in structure-II, are clearly seen using water mixed with lesser amount of THF.

Keywords: Gas hydrates, laboratory synthesis, Raman spectroscopy.

HUGE amounts of gas reserves are estimated in the form of gas hydrates across the world in deep-sea sediments and permafrost regions. Commercial production of just 15% of gas estimated from gas hydrates would provide the world with energy for 200 years at the current level of energy consumption[1]. Gas hydrates (clathrates) are the non-stoichiometric inclusion compounds encaging a small, normally apolar (guest) gaseous molecule (CH_4, C_2H_6, C_3H_8, CO_2, H_2S, etc.) in the framework of hydrogen-bonded, ice-like host molecules, and exist as a stable solid phase at high gas pressures and/or low temperatures. The ultimate concern of these hydrates is for alternate energy resources. This form of energy is more preferred as it has lesser pollutants. Even though huge amounts of natural gas are trapped in the condensed form (typically 1 m^3 of gas hydrate has STP equivalent methane of 163 m^3), its estimation, exploration and exploitation are not trivial; and more fundamental and technological aspects are to be addressed. Another concern is regarding the climatic impact of methane, a primary content of natural gas hydrates, and it has stronger greenhouse effects compared to carbon dioxide[2,3].

Three clathrate hydrate structures are commonly known[3], identified by the symbols sI, sII, and sH; existence of sH structure was confirmed more recently and this extended the size of the largest possible guests. Structure I can host small molecules such as methane, ethane and carbon dioxide, while structure II can also host larger molecules such as propane and isobutane. The cubic sI cell contains 46 H_2O molecules, two 12-hedra (5^{12}) and six 14-hedra ($5^{12}6^2$); where 5^{12} is used to indicate that the polyhedron contains 12 five-membered ring faces. The cubic sII cell contains 136 water molecules, eight large ($5^{12}6^4$), and sixteen small (5^{12}) cages (Table 1).

Methane molecules preferably occupy and stabilize the 5^{12} cavities by virtue of their molecular size. However, in pure methane hydrates, they are also contained in $5^{12}6^2$ cavities of sI. Carbon dioxide or ethane occupies predominantly the $5^{12}6^2$ cavities of sI. Propane molecules stabilize the $5^{12}6^4$ cavities of sII, while the smaller cavities are left empty and, therefore, not stabilized by the gas; as a consequence the maximum gas content of propane hydrate is inferior with respect to methane and ethane hydrates. Natural gas mixtures containing propane usually form sII hydrates. In the same way, if a substance with a suitable molecular diameter, such as tetrahydrofurane (THF; sII former occupying $5^{12}6^4$ cavities) is added to the water/methane system, an sII hydrate may form[3–5].

In this communication we report the characteristic Raman features of some hydrate formers, namely propane and methane; also variations using mixed systems (THF + methane). The gas hydrates were synthesized in the laboratory environment using indigenously developed pressure vessels. Raman investigations on laboratory-synthesized gas hydrates are being carried out worldwide[6–9]. Establishing the characteristic signatures of gas hydrates in our laboratories are of immense use, as this technique has been recognized as one of the tools in establishing the presence of gas in gas hydrates.

Micro-Raman measurements were carried out using 514.5 nm radiation from an air-cooled argon ion (Spectra Physic) laser. The scattered light was dispersed through a JY-T64000 triple monochromator system operating in subtractive mode, attached to a liquid nitrogen-cooled CCD detector. The Raman bands (stronger and sharper) are reproducible with ± 1 cm^{-1} uncertainty, whereas it could be up to ± 5 cm^{-1} for weaker and broader bands. The scattered light was detected in backscattered geometry using Jobin Yvon confocal microanalysis system attached with Olympus microscopy (model U-LH 100/3). The observed profiles were fitted into several components using GRAMS/3 software and best-fitted parameters were used in data interpretations. Temperature dependence measurements were performed by placing the sample inside the LINKAM FTIR-600 liquid nitrogen-cooled cryostat, which was placed under the confocal microscope of the Raman system. The temperature stability of the cryostat was better than ± 0.2 K.

Gas hydrates were synthesized in two different pressure cells, one with a capacity of about 2 ml and another

*For correspondence. (e-mail: psrprasad@ngri.res.in)

Table 1. Structural properties of clathrate hydrates (data compiled from Sloan Jr.[3])

	Structure I		Structure II		Structure H		
Hydrate type	S	L	S	L	S	M	L
Cavity	5^{12}	$5^{12}6^2$	5^{12}	$5^{12}6^4$	5^{12}	$4^35^66^3$	$5^{12}6^8$
Cavities/unit cell	2	6	16	8	3	2	1
Average cavity radius (Å)	3.95	4.33	3.91	4.73	3.91	4.06	5.71
Crystal class	Cubic		Cubic		Hexagonal		
Space group	Pm3n		Fd3m		P6/mmm		
Water molecules/unit cell	46		136		34		

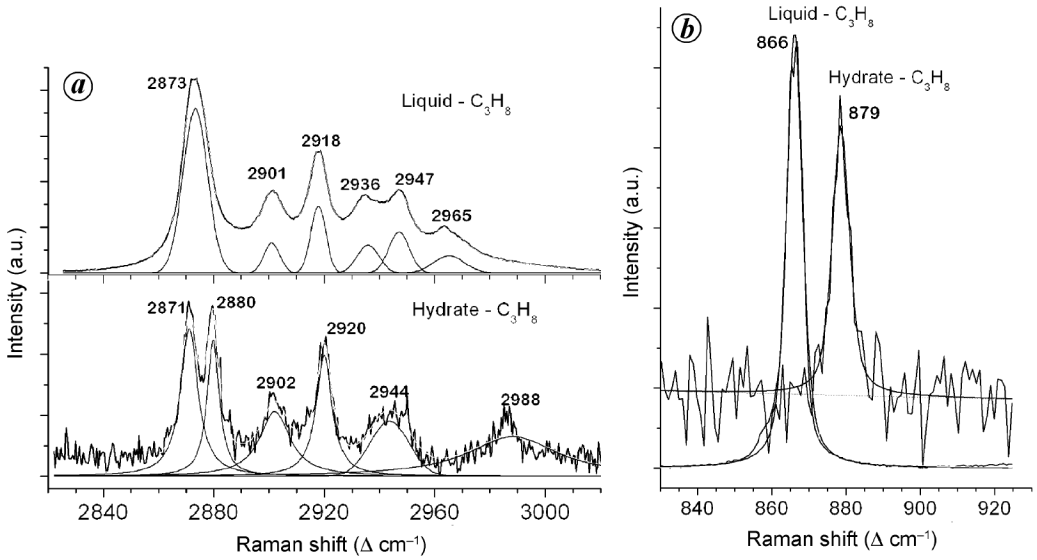

Figure 1. Raman spectra of propane in hydrate (recorded at 200 K and ambient pressure) and liquid (recorded at 300 K and ambient pressure) phases in the CH stretching (***a***) and bending mode (***b***) regions.

with about 46 ml. Both the cells were tested for possible gas leakages up to 10 MPa and were working satisfactorily even at 250 K. A micro-cell was fitted with an optical window (fused quartz) for probing the hydrate in its *in situ* formation condition. The cell was partially filled with de-ionized and de-gased water and charged with methane (8 MPa) or propane (1 MPa) for synthesizing gas hydrates. The cell was kept at about 260 K with intermittent stirring to initiate nucleation of hydrates. Growth of hydrates is nearly completed in about 4–5 days. Raman spectra were collected at lower temperatures by immersing the cell in liquid nitrogen. Another cell (46 ml) was used for bulk and mixed hydrate synthesis. After hydrate formation, the cell was cooled to temperatures lower than 180 K and then excess gas was removed from the reactor vessel. The hydrate samples were transferred onto the LINKAM stage to collect the Raman spectra.

Pure propane hydrates (sII hydrates) nucleate at relatively lower pressures. In fact, the quadruple points Q_1 and Q_2 are (273.1 K, 0.172 MPa) and (278.8 K, 0.556 MPa) respectively[3]. Thus the solid propane hydrate phase should be grown at higher pressures and sub-ambient temperatures. Initially the micro-cell (2 ml) was charged with 0.7 MPa gas and the temperature was decreased to 280 K. The cell was again charged with propane until a thinner layer was clearly seen. The mixture was thoroughly mixed by shaking intermittently and hydrates were clearly observed in about 48 h when kept under super-cooled conditions. Figure 1 shows the Raman spectra of hydrate and liquid propane in both CH stretching (Figure 1 *a*) and bending (Figure 1 *b*) mode regions. The Raman bands in liquid phase are broader compared to the hydrate phase and the stronger band at 2873 cm^{-1} splits into two (2871 and 2880 cm^{-1}) in the hydrate phase. Additionally, the weaker doublet (2936 and 2947 cm^{-1}) merged (2944 cm^{-1}) in the hydrate phase. Another characteristic Raman variation is in the CH bending mode region (Figure 1 *b*), where the band in the hydrate phase is up-shifted by 13 cm^{-1} (hydrate phase 879 cm^{-1} and liquid phase 866 cm^{-1}). All these observations are in agreement with earlier re-

Table 2. Fitted Raman peak parameters of gas hydrates in lattice modes with different guest molecules

Guest molecule	Observed Raman parameters (cm^{-1})		Hydrate structure
	Peak position (fwhm)	Peak position (fwhm)	
THF	219 (27)	66 (10)	sII
Propane	211 (29)	62 (6)	sII
CH_4 + THF	219 (20)	62 (4)	sII
Ethylene oxide	214 (28)	–	sI
Methane	213 (24)	–	sI
Carbon dioxide	208 (28)	–	sI
Ice	225 (10)	–	–

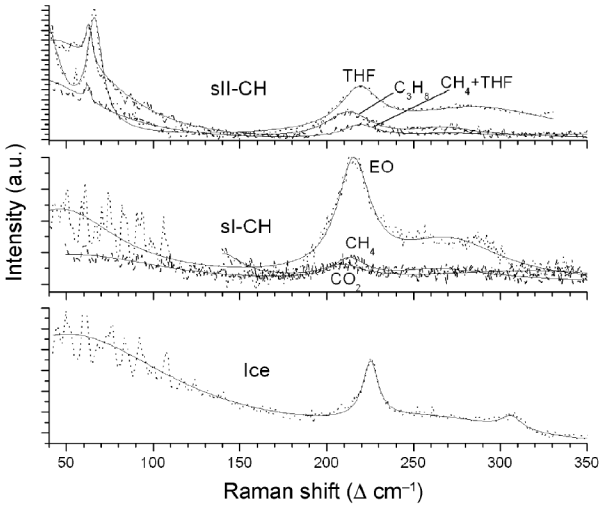

Figure 2. Low-frequency Raman spectra of some sI and sII forming systems compared with ice.

ports[6,10,11]. We synthesized propane hydrates as a first step in our experimental programme, and characterized them using Raman spectroscopy because the formation of these hydrates is at relatively lower pressures; and thus pressure vessels could be developed conveniently. Also, the characteristic features for pure propane hydrates were reported by lesser number of research groups and such measurements are needed as a benchmark for us before attempting measurements on methane hydrates.

The Raman spectra in the lower wavenumber region in gas hydrates comprising water lattice modes have also shown remarkable variations depicting disorder effects[12–15]. The Raman bands in this region were reported to have closer resemblance with ice Ih spectrum[16]. The Raman spectra of sI and sII hydrates in the lattice mode region were compared with ice at 90 K (Figure 2). All spectra were recorded under identical experimental conditions. The fitted parameters, namely peak positions and half-widths are shown in Table 2. The spectrum of ice has a sharper (fwhm 10 cm^{-1}) band at 225 cm^{-1}, with an additional broad and weaker mode around 306 cm^{-1}. The spectral features in clathrate (sI and sII) are similar to ice, with the exception that the bandwidth of the stronger intermolecular O–O stretching mode is much higher (28 cm^{-1}). A small variation of 4 cm^{-1} is observed in the peak position of this mode between sI and sII structures. However, it is difficult to consider this as significant because the bands are weaker and broader. Nevertheless, the lattice mode and its broader nature could be useful in identifying the formation of hydrates. Additionally, a sharper mode at 60 cm^{-1} is clearly observed in THF, propane and (CH_4 + THF) clathrates, which are sII clathrate hydrate formers. No such peak has been reported for ice[16] and thus could be a characteristic feature of sII hydrates. The low-frequency Raman spectral feature reported here broadly agrees with earlier reports[13–15] and this region was probed, in various gas molecules as guests. In the Raman spectroscopic studies in the lattice mode region (140–350 cm^{-1}), covering intermolecular O–O vibration, various gas-hydrate systems were reported at higher pressures[17,18] up to 500 MPa. A linear shift with increasing pressures has been reported and the rate of shift depends on the guest molecules[17,18]. Our results indicate that the broad features of the stretching vibrations of ice (host) observed at around 220 cm^{-1} could be characteristic of gas hydrates and the low-frequency mode at around 60 cm^{-1} could be a fingerprint of sII.

Methane is the major hydrocarbon in naturally occurring gas hydrates and the Raman spectroscopy has distinctly different spectral signatures[6–9]. Hence it is one of the useful experimental techniques for establishing the presence of methane hydrates. In Figure 3 the characteristic Raman spectra of methane hydrates, synthesized in the laboratory is shown. Two peaks were fitted in the observed spectral segment in the Raman range 2880–2940 cm^{-1}. The fitted peaks were at 2905 and 2917 cm^{-1} and are due to methane molecules occupied in the larger and smaller cages of sI. We observed one band around 2918 cm^{-1} for methane in gaseous phase. We noticed that 2917 cm^{-1} is about two wavenumbers higher than that reported in the literature[6–9], which could be due to a combination of poor S/N ratio (due to triple-stage configuration used in our experimental set-up) and/or residual CH_4 in the pressure vessel. Nevertheless, the present results are broadly comparable with the reported data[6–9] and these

studies serve as a good laboratory scale while probing natural hydrates. The number of $5^{12}6^2$ (large) and 5^{12} (small) cages in sI is 6 and 2 respectively (Table 1). Therefore, Raman intensity for the 2905 cm^{-1} mode should be three times that of 2917 cm^{-1}, if the cages are fully occupied with methane gas and this ratio is observed to be 3.48.

It would be interesting to study the occupancy of methane molecules in sII-forming hydrate system. In sII hydrates, e.g. THF and propane, larger cages ($5^{12}6^4$) were occupied by THF/C_3H_8 and the smaller cages (5^{12}) were empty. Small molecules such as CH_4, when present in mixed systems (e.g. natural gas), can occupy smaller cages. We synthesized methane hydrates using different ratios of aqueous THF in 46 ml P, T vessel, as described earlier. The Raman spectra were recorded at 175 K using LINKAM stage. Spectral features in 2880–2940 cm^{-1} are shown in Figure 4. Water to THF mixtures in our studies were 17 and 34 (mol). In other words, the resultant THF hydrates will be with fully (8) and half (4) occupied large cages; the small (16) cages are empty and methane molecules can occupy them. We previously reported some subtle variations in Raman spectral features for pure THF hydrates[13]. Similar spectral signatures were also observed in the present study, i.e. weaker Raman bands were observed at 2720, 2864 and 2877 cm^{-1} and also at 2942 and 2985 cm^{-1}, corroborating THF as a co-guest[13]. In the present study we discuss the behaviour of C–H vibrations of methane molecules. There is only one Raman mode around 2915 cm^{-1}, corresponding to methane molecules in small cages, in hydrates formed from 1 : 17 mol ratios of THF : H_2O (Figure 4, top). On the other hand, two modes at 2915 and 2905 cm^{-1} are clearly seen when the THF : H_2O mol ratio is 1 : 34. The additional mode at 2905 cm^{-1} corresponds to the methane molecules occupying larger cages of sII. One can distinguish sI and sII structures from the relative variations of peaks corresponding to small and large cages. As can be seen from Table 1, the number of small and large cages in sI is 2 and 6 and the same in sII is 16 and 8. Therefore, the Raman intensity for the corresponding modes should be (1 : 3) for sI and (2 : 1) for sII. Usually methane hydrates stabilize in sI and the observed Raman intensity ratio for small to large cages 1 : 3.48, closely agrees with the ideal sI structure. On the other hand, Raman signatures in mixed hydrates (guest molecules being THF and CH_4) need attention. There is no band in the CH-stretching region of methane corresponding to larger cages in THF : H_2O at 1 : 17 mol ratio (Figure 4). We observed that this band progressively became weaker and disappeared around 283 K, indicating the dissociation of hydrates. Two bands at 2915 and 2905 cm^{-1} are clearly seen when the THF : H_2O mol ratio is 1 : 34 and the mode at 2905 cm^{-1} is due to larger cages ($5^{12}6^4$) of sII (Figure 4, bottom). Comparison between Figures 3 and 4 demonstrates the Raman characteristic of methane hydrate in sI and sII with both types of cage occupancy. However, the observed intensity ratio for small to large cages is around 4, and is much higher than the ideal case. This is because only four larger cages were available for methane molecules, with the remaining four were being occupied by THF in the aqueous mixture used in our studies.

In summary, we have synthesized gas hydrates and characterized them using micro Raman spectroscopy. Observed Raman signatures in methane and propane hydrates corroborate reported results. We have also established that a Raman mode around 60 cm^{-1} is a characteristic feature of sII hydrates. With these measurements we are now fully equipped to analyse hydrate-bearing natural sediments in the country. We have also established the

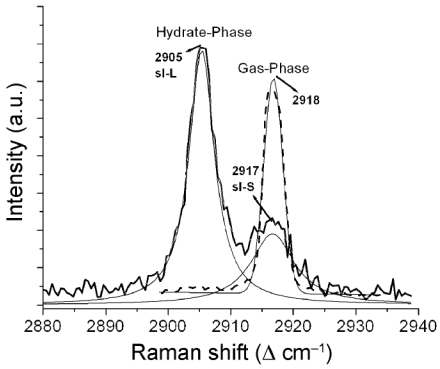

Figure 3. Characteristic Raman spectrum of methane hydrates recorded (at 200 K and 5 MPa) in CH stretching mode region. The Raman signature for gas phase is also shown.

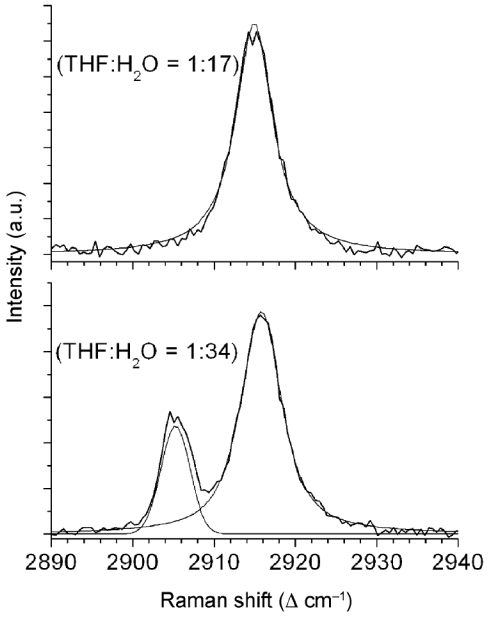

Figure 4. Characteristic Raman spectrum of methane hydrates in sII synthesized using (THF + H_2O) mixture in 1 : 17 mol (top) and 1 : 34 mol (bottom). Raman spectra were recorded at 175 K and ambient pressure.

signatures of methane hydrates in both sI and sII structures.

1. Makogon, Y. F., Holditch, S. A. and Makogon, T. Y., Natural gas-hydrates – A potential energy source for the 21st century. *J. Pet. Sci. Eng.*, 2007, **56**, 14–31.
2. Sloan, E. D., Introductory overview: Hydrate knowledge development. *Am. Mineral.*, 2004, **89**, 1155–1161.
3. Sloan Jr, E. D., *Clathrate Hydrates of Natural Gases*, Marcel Dekker, New York, 1998.
4. Fleyfel, F. and Devlin, J. P., Carbon dioxide clathrate hydrate epitaxial growth: Spectroscopic evidence for formation of the simple type-II CO_2 hydrate. *J. Phys. Chem.*, 1991, **95**, 3811–3815.
5. Prasad, P. S. R., Shiva Prasad, K. and Thakur, N. K., FTIR signatures of type-II clathrates of carbon dioxide in natural quartz veins. *Curr. Sci.*, 2006, **90**, 1544–1547.
6. Sum, A. K., Burrus, R. C. and Sloan, E. D., Measurement of clathrate hydrates via Raman spectroscopy. *J. Phys. Chem. B*, 1997, **101**, 7371–7377.
7. Uchida, T. *et al.*, Spectroscopic observations and thermodynamic calculations on clathrate hydrates of mixed gas containing methane and ethane: Determination of structure, composition and cage occupancy. *J. Phys. Chem.*, 2002, **106**, 12426–12431.
8. Seo, Y., Lee, H. and Ryu, B., Hydration number and two-phase equilibria of CH_4 hydrate in the deep ocean sediments. *Geophys. Res. Lett.*, 2002, **29**, 85-1–85-4.
9. Schicks, J. M. and Ripmeester, J. A., The coexistence of two different methane hydrate phases under moderate pressure and temperature conditions: kinetic versus thermodynamic products. *Angew. Chem. Int. Ed., Engl.*, 2004, **43**, 3310–3313.
10. Uchida, T. *et al.*, Two-step formation of methane–propane mixed gas hydrates in a batch-type reactor. *AIChE J.*, 2004, **50**, 518–523.
11. Schicks, J. M., Naumann, R., Erzinger, J., Hester, K. C., Koh, C. A. and Sloan, E. D., Phase transitions in mixed gas hydrates: Experimental observations versus calculated data. *J. Phys. Chem.*, 2006, **110**, 11468–11474.
12. Schicks, J. M., Erzinger, J. and Zieman, M. A., Raman spectra of gas hydrates – Differences and analogies to ice 1h and (gas saturated) water. *Spectrochim. Acta A*, 2005, **61**, 2399–2403.
13. Prasad, P. S. R., Prasad, K. S. and Thakur, N. K., Laser Raman spectroscopy of THF clathrate hydrate in the temperature range 90 to 300 K. *Spectrochim. Acta A*, 2007, **68**, 1096–1100.
14. Takasu, Y., Iwai, K. and Nishio, I., Low frequency Raman profile of type II clathrate hydrate of THF and its application for phase identification. *J. Phys. Soc. Jpn.*, 2003, **72**, 1287–1291.
15. Takasu, Y. and Nishio, I., New analysis of low frequency Raman spectra of THF aqueous solution and its co-existing phase with clathrate hydrate. *J. Phys. Soc. Jpn.*, 2003, **72**, 2106–2109.
16. Li, J. and Ross, D. K., Evidence of two kinds of H-bonds in ice. *Nature*, 1993, **365**, 327–329.
17. Sugahara, K., Tanaka, Y., Sugahara, T. and Ohgaki, K., Thermodynamic stability and structure of nitrogen hydrate crystal. *J. Supramol. Chem.*, 2002, **2**, 365–368.
18. Sugahara, K., Sugahara, T. and Ohgaki, K., Thermodynamic and Raman spectroscopic studies of Xe and Kr hydrates. *J. Chem. Eng. Data*, 2005, **50**, 274–277.

ACKNOWLEDGEMENTS. We are indebted to Prof. H. K. Gupta, Rajaramanna Fellow and Dr P. S. Goel, Secretary, Ministry of Earth Science Systems, Government of India for their keen interest and encouragement. We thank the Director, National Geophysical Research Institute, Hyderabad, for encouragement. We also thank Mr B. Satyanarayana for providing technical support in the fabrication of pressure vessels and the anonymous reviewers for stimulating suggestions on the manuscript.

Received 18 July 2007; revised accepted 24 April 2008

Understanding the suspended sediment dynamics in the coastal waters of the Bay of Bengal using high resolution ocean colour data

P. N. Sridhar*, I. V. Ramana, M. M. Ali and B. Veeranarayana

National Remote Sensing Agency, Department of Space, Balanagar, Hyderabad 500 625, India

The suspended sediment concentration (SSC) in the coastal ocean of the Bay of Bengal (BOB) is retrieved with high-resolution ocean colour data of the Ocean Colour Monitor (OCM) on-board satellite Oceansat-I. The SSC distribution in the coastal waters of the BOB has a regional gradient from north to south that follows the general monsoon circulation of the east coast of India. However, factors like tidal, fluvial and long shore currents play a major role in the regional sediment dynamics with understandable source, sink and pathway. In addition, other influences like geostrophic currents in the coastal sediment transport and dynamics are evident from the ocean colour data.

Keywords: Coastal waters, geostrophic currents, ocean colour data, suspended sediment dynamics.

SUSPENDED sediments play a major role in the coastal ocean turbidity, water quality, estuarine, tidal inlet, coral reef and mangrove ecosystem sedimentation excreta[1,2]. Therefore, coastal sediment transport and dynamics are central to the analysis and prediction of environmental quality, habitat stability, public-health risks, marine hazards such as ship-grounding, access to ports, seabed scouring, siltation of harbours and coastal protection[3]. The sediment dispersal system in the shelf of the Bay of Bengal (BOB) characterizes substantial temporal and spatial variability, as it is driven by major rivers[4], namely the Ganges, Brahmaputra, Bramani, Baitarani, Mahanadi, Krishna, Godavari, Pennar and Cauvery from high-altitude mountains and hence has national and global significance.

Sediment distribution in the coastal ocean water column may occur either as a diffusive process, where the bed is flat and devoid of bed forms[5] or as a convective process[6]. The sediment is also suspended and lifted upward in coherent pockets due to vortex shedding from ripples at the bed. The amount of sediment suspended depends on bed elevation, configuration, bed shear stress and wave breaker[7]. Winds drive water along the inner shelf and ocean circulation system forces the outer-shelf water movements. In the inner-shelf, the wave boundary layer thickness is smaller than current boundary layer

*For correspondence. (e-mail: sridhar_pn@nrsa.gov.in)